Mechanics and Mechanical Engineering
Vol. 19, No. 2 (2015) 91–101

Parametric Optimization and Interaction Effect of TIG Welding Parameters for Stainless Steel (SS 301) Sheets

M. Pandi Krishnan
Department of Mechanical Engineering
Chendhuran College of Engineering & Technology
Pudukkottai–622 507

A. Naveen Sait
Department of Mechanical Engineering
Chendhuran College of Engineering and Technology
Lena VIlakku, Pilivalam Post, Pudukkottai District
Tamil Nadu, India
naveensait@yahoo.co.in

Received (11 August 2015)
Revised (16 September 2015)
Accepted (22 December 2015)

In the present work, TIG welding process parameters were optimized for joining 301 stainless–steel plates. Welding pressure, welding speed and welding temperature combinations were carefully selected with the objective of producing weld joint with maximum impact strength and hardness. Taguchi technique was applied for optimizing the selected welding parameters. The factors used in this study consisted of pressure, welding speed and welding temperature, each of which had three levels in the study. L_{27} orthogonal array was selected according to the aforementioned factors and levels and experimental tests were performed. Signal-to-noise (SN) ratio was used to evaluate the experimental results. The results indicate that the welding speed has the greatest influence on impact strength, followed by welding pressure and temperature. Experiments have also been conducted to validate the optimized parameters.

Keywords: TIG welding, Taguchi, Stainless steel, Optimization.

1. Introduction

Welding is the joining of materials in the welding zone with the use of heat and force, with or without filler metal. It can be facilitated with the help of, for example, shielding gases, welding powders, or pastes. However the energy required for welding is supplied by an esteemed source. TIG welding is a process that produces a weld at the surfaces of two similar metals. Like spot welding, seam welding relies

on two electrodes, usually made from copper, to apply pressure and current. The electrodes are disc shaped and rotate as the material passes between them. This allows the electrodes to stay in constant contact with the material to make long continuous welds. The electrodes may also move or assist the movement of the material. TIG welding is a continuous joining process using electrode wheels on generally overlapping work pieces. The Taguchi method is one of the techniques that could be applied to optimize the input welding parameters. Optimization of process parameters is the key step in the Taguchi method in achieving high quality, without increasing the cost [1]. Sathiya et al carried out on 3.5kW cooled slab laser welding of 904 L super austenitic stainless steel. The joints have butts welded with different shielding gases, namely argon, helium and nitrogen, at a constant flow rate. Super austenitic stainless steel (SASS) normally contains high amount of Mo, Cr, Ni, N and Mn [2]. Yang dongxia studies the Optimization of weld bead geometry in laser welding with filler wire process using Taguchi's approach It supports to improve productivities and decrease the time required for the experimental investigation, so that high–quality products can be created quickly and at low cost [3]. Generally, the quality of a weld joint is directly influenced by the welding input parameter settings. Selection of proper process parameters is important to obtain the desired weld bead profile and quality. Reisgen et al carried out work on numerical and graphical optimization techniques of the CO_2 laser beam welding of dual phase transformation induced plasticity steel sheets using response surface methodology (RSM) based on Box–Behnken design. They have established procedure to improve the weld quality, increase the productivity and minimize the total operation cost by considering the welding parameters range of laser power, welding speed and focus position. It was found that, RSM can be considered as a powerful tool in experimental welding optimization, even when the researcher does not have a model for the process [4]. RanfengQiu et al joined aluminum alloy A5052 cold–rolled steel plates and austenitic stainless steel SUS304 using resistance spot welding with a cover plate. They observed interfacial microstructure using transmission electron microscope [5]. Khan et al investigated the effects of energy density on geometry of the weld seam and development of microstructures at various weld zones. Energy–based local micro ardness profiles are made and linked with the formation of the microstructures. Weld resistance at the interface is energy–limited and seam profile only changes from conical to cylindrical after a certain limit of energy input [6]. Danial Kianersi et al optimized welding parameters namely welding current and time in resistance spot welding of the austenitic stainless steel sheets of grade AISI 316L. They also investigated the effect of optimum welding parameters on the resistance spot welding properties and microstructure of AISI 316L austenitic stainless steel sheets [7]. Tomasz Sadowski et al obtained hybrid joints, a combination of two simple techniques, e.g. by spot welding and adhesive, are relatively modern joints developed especially for application in aerospace industry. This contribution describes the modeling and testing of structural elements by application of an angle bar and spot welding techniques with the introduction of adhesive layers between adherents [8]. R.S.Florea et al investigated the fatigue behavior of resistance spot welding in aluminum 6061–T6 alloy. They included the process optimization of the forces, currents and times for main weld and post–heating [9]. Wei and Wu et al studied that the effects of local electrical contact resistance on transport variables,

cooling rate, solute distribution, and nugget shape after solidification responsible for microstructure of the fusion zone during resistance spot welding are realistically and systematically investigated [10]. Mustafa Kemal et al studied that the friction stir spot welding parameters affect the weld strength of thermoplastics, such as high density polyethylene (HDPE) sheets. The strength of a friction stir spot weld is usually determined by a lap–shear test [11].

In the present work, Taguchi's technique is employed to determine the influence of the resistance Tig welding with input parameters (Pressure, Speed and Temperature) on the hardness and the impact strength of the weld joints. The emphasis is focused on the optimization of the welding parameters, in order to maximize both the hardness and the impact strength.

2. Experimental details

2.1. *Materials*

The material used in this investigation was AISI 301 stainless steel and dimensions of 100 mm × 50 mm × 1.2 mm each were used as work–piece materials. The chemical compositions of the material used are shown in Tab. 1. The joints were produced using Tig welding process with welding parameters and levels as described in Table 2. The welded specimens are presented in Fig. 1. Specimens for the mechanical testing were prepared as per ASTM standards. The hardness test for weld region was tested by using Brinell and Rockwell hardness testing machine. The applied force was 1000 N and 10 mm diameter ball indentor was used in Brinell hardness testing machine. In Rockwell hardness testing machine the load was 100 kg and 0.0625 mm diameter ball indentor was used. The indentation after testing was measured using optical microscope. The standard formula was used to calculate the Brinell Hardness Number (BHN) and Rockwell hardness Number (RHN). The impact strength of the weld joints were determined using Izord specimen. The standard Izord test specimens were prepared for the test.

Table 1 Composition ranges for 301 grade stainless steel

Grade		C	Mn	Si	P	S	Cr	Ni	N
301	min.	-	-	-	-	-	16.0	6.0	-
	max.	0.15	2.0	1.0	0.045	0.030	18.0	8.0	0.10

2.2. *Plan of Experiments*

Taguchi approach was used for designing the experiments, L27 orthogonal array was applied which composed of three columns and 27 rows, which mean that 27 experiments were carried out. DOE was selected based on a three welding parameters with 3 levels each. The selected welding parameters for this study are: welding pressure, welding speed and temperature. Tab. 2 shows the input variables and experiment design levels. Taguchi method was applied to the experimental data using statistical software MINITAB 15. The SN ratio for each level of process parameters is computed based on the SN analysis. Regardless of the category of the

quality characteristic; a higher SN ratio corresponds to a better quality characteristic. Therefore, the optimal level of the process parameter is the level with the highest SN ratio.

Furthermore, a statistical analysis of variance (ANOVA) is performed for each response individually to see which process parameters are statistically significant. The optimal combination of the process parameters can then be predicted.

Table 2 Process parameters and their levels

Factor	Unit	Type	Level	Values		
Press	MPa	Fixed	3	5.884	7.845	9.806
Speed	Rpm	Fixed	3	30	45	60
Temp	^{0}C	Fixed	3	40	50	60

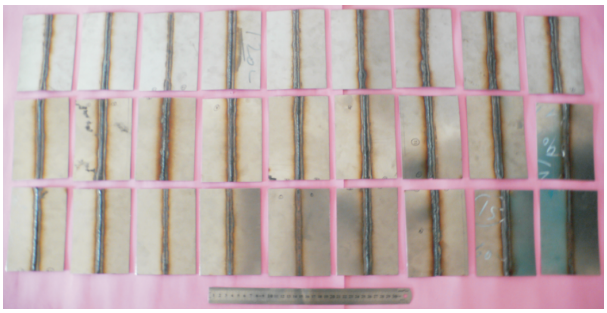

Figure 1 Photograph showing the welded specimens

3. Results and Discussion

In this study, an L_{27} orthogonal array with 3 columns and 27 rows was used. Twenty seven experiments were required to study the welding parameters using L_{27} orthogonal array. The experimental layout for the welding process parameters using the L_{27} orthogonal array is shown in Tab. 3. The responses for signal–to–noise ratio are presented in Tab. 4. Design expert 7 software was used for analyzing the measured responses.

3.1. *The signal–to–noise (SN) ratio analysis*

In order to evaluate the influence of each selected factor on the responses, The signal–to–noise ratios SN for each factor is to be calculated. The signals have indicated that the effect on the average responses and the noises were measured by the influence on the deviations from the average responses, which would indicate the sensitiveness of the experiment output to the noise factors. The appropriate SN ratio must be chosen using previous knowledge, expertise, and understanding of the process. When the target is fixed and there is a trivial or absent signal factor (static

Table 3 Experimental layout – L_{27} orthogonal array

Exp. No	**Input Parameters**			**Pressure (MPa)**	**Speed (rpm)**	**Temp (°C)**
	A	**B**	**C**			
1	1	1	1	5.884	30	40
2	1	2	2	5.884	45	50
3	1	3	3	5.884	60	60
4	2	1	1	7.845	30	40
5	2	2	2	7.845	45	50
6	2	3	3	7.845	60	60
7	3	1	1	9.806	30	40
8	3	2	2	9.806	45	50
9	3	3	3	9.806	60	60
10	3	1	2	9.806	30	50
11	3	2	3	9.806	45	60
12	3	3	1	9.806	60	40
13	1	1	2	5.884	30	50
14	1	2	3	5.884	45	60
15	1	3	1	5.884	60	40
16	2	1	2	7.845	30	50
17	2	2	3	7.845	45	60
18	2	3	1	7.845	60	40
19	2	1	3	7.845	30	60
20	2	2	1	7.845	45	40
21	2	3	2	7.845	60	50
22	3	1	3	9.806	30	60
23	3	2	1	9.806	45	40
24	3	3	2	9.806	60	50
25	1	1	3	5.884	30	60
26	1	2	1	5.884	45	40
27	1	3	2	5.884	60	50

design), it is possible to choose the SN ratio depending on the goal of the design. In this study, the SN ratio was chosen according to the criterion the "larger is better", in order to maximize the responses. The SN ratio for the "larger is better" target for all the responses was calculated as follows [11].

Larger the better:

$$S/N\text{ratio} = -10\log_{10}\frac{1}{n}\sum_{i=1}^{n}\frac{1}{y_i^2}$$

where:

n – number of variables,

y_i – the value of the response.

Using the above presented data with the selected above formula for calculating

Table 4 Response methodology parameters

Exp. No	**Input parameters**			**Response Value**			**S/N ratio**		
	Pressure (MPa)	**Speed (rpm)**	**Temp (°C)**	**Impact**	**BHN**	**RHN**	**Impact**	**BHN**	**RHN**
1	5.88	30.00	40.00	1.16	132.09	94.33	1.16	1.25	1.25
2	5.88	45.00	50.00	1.21	106.86	75.33	1.21	1.25	1.25
3	5.88	60.00	60.00	0.96	135.15	72.66	0.96	1.25	1.25
4	7.85	30.00	40.00	1.09	118.77	87.00	1.09	4.26	4.26
5	7.85	45.00	50.00	0.96	152.41	93.00	0.96	4.26	4.26
6	7.85	60.00	60.00	0.92	151.65	74.00	0.92	4.26	4.26
7	9.81	30.00	40.00	0.77	171.41	85.00	0.77	5.15	5.15
8	9.81	45.00	50.00	0.86	144.75	78.00	0.86	5.15	5.15
9	9.81	60.00	60.00	0.96	138.21	71.33	0.96	5.15	5.15
10	9.81	30.00	50.00	0.72	141.38	81.33	0.72	4.26	4.26
11	9.81	45.00	60.00	0.54	138.15	79.00	0.54	4.26	4.26
12	9.81	60.00	40.00	0.96	144.75	94.33	0.96	4.26	4.26
13	5.88	30.00	50.00	0.82	141.41	84.66	0.82	8.16	8.16
14	5.88	45.00	60.00	0.71	121.07	73.66	0.71	8.16	8.16
15	5.88	60.00	40.00	0.67	109.03	81.66	0.67	8.16	8.16
16	7.85	30.00	50.00	0.83	163.05	93.66	0.83	4.68	4.68
17	7.85	45.00	60.00	1.26	141.38	80.33	1.26	4.68	4.68
18	7.85	60.00	40.00	1.09	138.09	82.33	1.09	4.68	4.68
19	7.85	30.00	60.00	0.89	163.05	86.66	0.89	5.15	5.15
20	7.85	45.00	40.00	0.79	135.15	76.00	0.79	5.15	5.15
21	7.85	60.00	50.00	1.21	123.67	74.33	1.21	5.15	5.15
22	9.81	30.00	60.00	1.05	100.65	72.33	1.05	4.68	4.68
23	9.81	45.00	40.00	0.56	185.11	78.33	0.56	4.68	4.68
24	9.81	60.00	50.00	0.60	151.65	84.66	0.60	4.68	4.68
25	5.88	30.00	60.00	1.16	148.14	78.33	1.16	9.28	9.28
26	5.88	45.00	40.00	1.26	126.45	74.66	1.26	9.28	9.28
27	5.88	60.00	50.00	0.82	159.16	91.33	0.82	9.28	9.28

SN, the Taguchi experiment results are summarized in Tab. 5 and presented in Fig. 2, which were obtained by means of MINITAB 15 statistical software. It can be noticed from the Fig. 2 (the SN plot), the welding pressure (P) is the most important factor affecting the impact strength. Welding temperature (T) has a lower effect. Main effects plot for SN ratios suggest that those levels of variables would increase the impact strength of the weld joint.

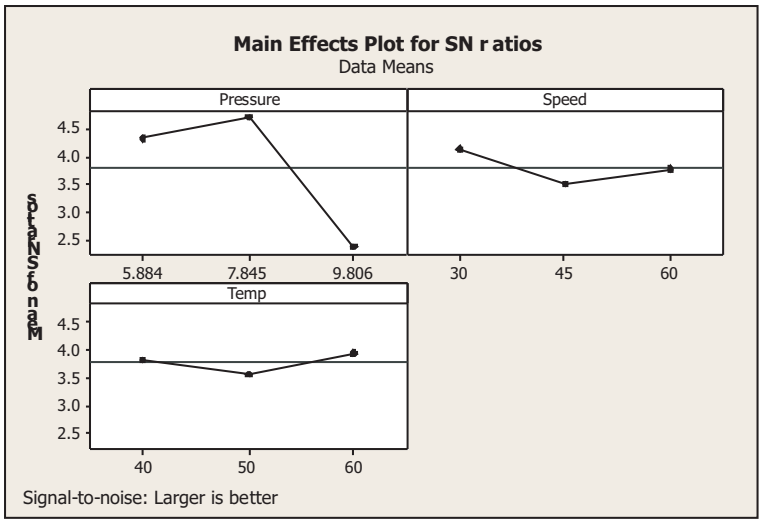

Figure 2 Main effects plot for SN ratios

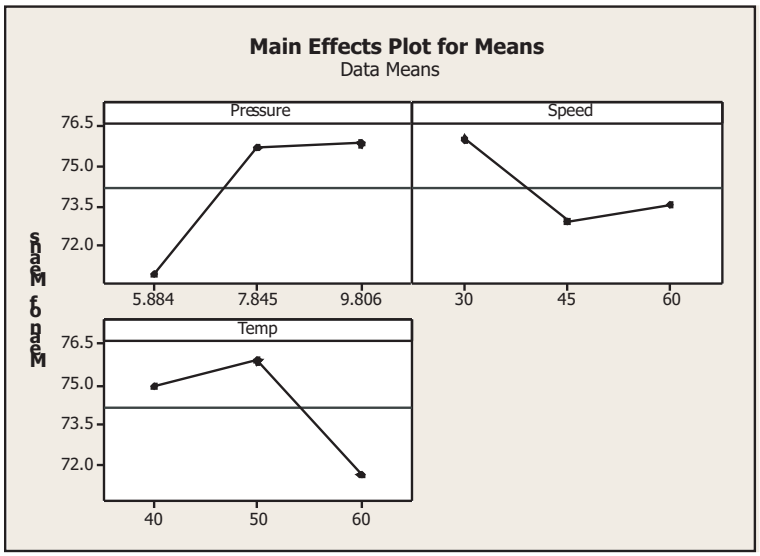

Figure 3 Main effects plot for means

Table 5 Response table for SN ratios

Level	Pressure MPa	Speed Rpm	Temp ^{0}C
1	4.311	4.114	3.827
2	4.696	3.487	3.575
3	2.357	3.764	3.964
Delta	2.339	0.628	0.389
Rank	1	2	3

Table 6 Response table for means

Level	Pressure MPa	Speed Rpm	Temp ^{0}C
1	70.92	75.99	74.92
2	75.69	72.88	75.88
3	75.83	73.56	71.64
Delta	4.91	3.11	4.24
Rank	1	3	2

3.2. *Interaction plot for SN ratio*

From the interaction plot shown in Fig. 4, it is observed that the interaction of SN ratio, the pressure value increases with respect to temperature. The SN ratio value increases with the increase in speed for moderate temperature. From the Fig. 3 and Tab. 6, it is observed that the welding pressure (P) is the most significant factor and the welding speed (S) is an insignificant factor for the hardness of the welding zone.

3.3. *Analysis of variance (ANOVA)*

The purpose of the ANOVA is to investigate which welding process parameters significantly affect the quality characteristic. This is accomplished by separating the total variability of the SN ratios, which is measured by the sum of the squared deviations from the total mean of the SN ratio, contributions by each welding process parameter and the error. The percentage contribution by each of the process parameter is the total sum of the squared deviations which is used to evaluate the importance of the process parameter change on the quality characteristic. In addition, the F test can also be used to determine which welding process parameters have a significant effect on the quality characteristic. Usually, the change of the welding process parameter has a significant effect on the quality characteristic when the F value is large [11].

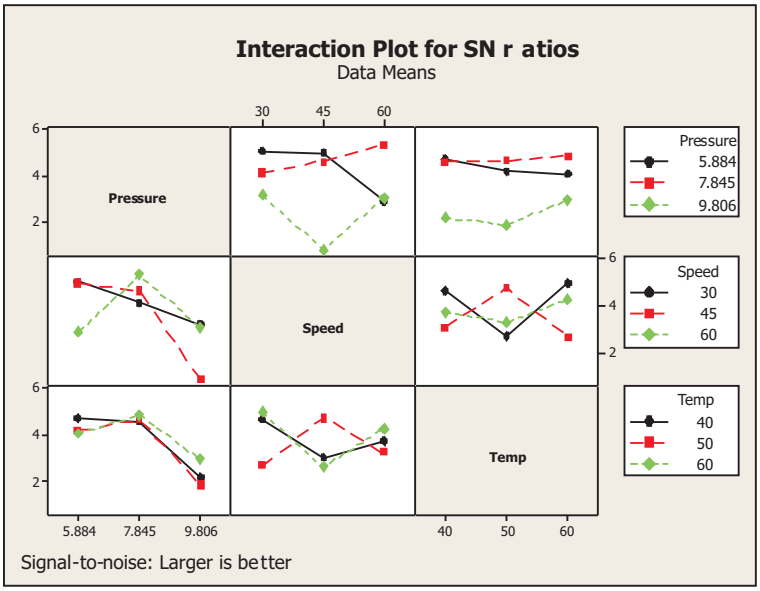

Figure 4 Interaction plot for SN ratios

3.4. *Analysis of variance for impact strength and hardness (BHN, RHN)*

The purpose of ANOVA is to find the significant factor statistically. It gives a clear picture as to how far the process parameter affects the response and the level of significance of the factor considered. The ANOVA table for mean and signal to noise ratio are calculated and listed in Tabs 7, 8 and 9. The F test is being carried out to study the significance of the process parameter. The high F value indicates that the factor is highly significant in affecting the response of the process. In our investigation, welding speed is a highly significant factor and plays a major role in affecting the impact strength of the weld. Welding temperature is the most significant factor affecting the hardness of weld zone.

Table 7 Analysis of variance for impact

Source	DF	SS	MS	F	P
Pressure	2	0.007595	0.003689	1.25	0.303
Speed	2	0.026515	0.013270	4.45	0.024
Temp	2	0.000070	0.000047	0.03	0.985
Error	20	0.056390	0.002918		
Total	26	0.092520			

S = 0.0540323 R-Sq = 36.82% R-Sq (adj) = 17.87%

Table 8 Analysis of variance for BHN

Source	DF	SS	MS	F	P
Pressure	2	168.75	83.86	0.96	0.394
Speed	2	32.49	16.27	0.18	0.829
Temp	2	168.32	84.65	0.97	0.391
Error	20	1710.63	86.07		
Total	26	2096.19			

S = 0.0640625 R-Sq = 39.62% R-Sq(adj) = 19.37%

Table 9 Analysis of variance for RHN

Source	DF	SS	MS	F	P
Pressure	2	169.75	83.86	0.95	0.393
Speed	2	32.49	16.27	0.18	0.827
Temp	2	168.33	85.64	0.97	0.399
Error	20	1710.63	86.07		
Total	26	2195.19			

S = 0.0750623 R-Sq = 40.66% R-Sq(adj) = 20.52%

4. Conclusions

From the present investigation the following conclusions are drawn:

1. The stainless steel sheets (301 Grade) are joined successfully using TIG welding process.

2. Welding pressure influences most on the impact strength of the weld joint among the selected parameters.

3. Weld zone hardness is affected by the factor of welding temperature during TIG welding of stainless steel sheets.

Taguchi's design method can be effectively used for optimizing the welding parameters.

References

[1] **Vural, M.**: Welding Processes and Technologies, *Compre. Mater. Proc.*, 6, pp. 3–48, DOI:10.1016/B978-0-08-096532-1.00601-4, **2014**.

[2] **Sathiya, P., Abdul Jaleel, M.Y., Katherasan, D. and Shanmugarajan, B.**: Optimization of laser butt welding parameters with multiple performance characteristics, *Opt. Laser Technol.*, 43, pp. 660–673, DOI:10.1016/j.optlastec.2010.09.007, **2011**.

[3] **Dongxia, Y., Xiaoyan, L., Dingyong, H., Zuoren, N. and Hui, H.**: Optimization of weld bead geometry in laser welding with filler wire process using Taguchi's approach, *Opt. Laser Technol.*, 44, pp. 2020–2025 DOI:10.1016/j.optlastec.2012.03.033, **2012**.

[4] **Reisgen, U., Schleser, M., Mokrov, O. and Ahmed, E.**: Optimization of laser welding of DP/TRIP steel sheets using statistical approach, *Opt. Laser Technol.*, 44, pp. 255–262, DOI:10.1016/j.optlastec.2011.06.028, **2012**.

[5] **Qiu, R., Iwamoto, C. and Satonaka, S.**: Interfacial microstructure and strength of steel/aluminum alloy joints welded by resistance spot welding with cover plate, *J. Mater. Proc. Tech.*, 209, pp. 4186–4193, DOI:10.1016/j.jmatprotec.2008.11.003, **2009**.

[6] **Khan, M. M. A., Romoli, L., Ishak, R., Fiaschi, M., Dini, G. and De Sanctis, M.**: Experimental investigation on seam geometry, microstructure evolution and micro hardness profile of laser welded martensitic stainless steels, *Opt. Laser Technol.*, 44, pp. 1611–1619, DOI:10.1016/j.optlastec.2011.11.035, **2012**.

[7] **Kianersi, D., Mostafaei, A. and Ali Amadeh, Ahmad**: Resistance spot welding joints of AISI 316L austenitic stainless steel sheets: Phase transformations, mechanical properties and microstructure characterizations, *Mater. Design.*, 61, pp. 251–263, DOI:10.1016/j.matdes.2014.04.075, **2014**.

[8] **Sadowski, T., Golewski, P. and Kneć, M.**: Experimental investigation and numerical modelling of spot welding–adhesive joints response, *Compos. Struct.*, 112, pp. 66–77, DOI:10.1016/j.compstruct.2014.01.008, **2014**.

[9] **Florea, R. S., Bammann, D. J., Yeldell, A., Solanki, K. N. and Hammi, Y.**: Welding parameters influence on fatigue life and microstructure in resistance spot welding of 6061-T6 aluminum alloy, *Mater. Design.*, 45, pp. 456–465, DOI:10.1016/j.matdes.2012.08.053, **2013**.

[10] **Wei, P. S. and Wu, T. H.**: Electrical contact resistance effect on resistance spot welding, *Int. J. Heat Mass Tran.*, 55, pp. 3316–3324, DOI:10.1016/j.ij heatmasstransfer.2012.01.040, **2012**.

[11] **Bilici, M. K., Ykler, A. I. and Kurtulmus, M.**: The optimization of welding parameters for friction stir spot welding of high density polyethylene sheets, *Mater. Design.*, 32, pp. 4074–4079, DOI:10.1016/j.matdes.2011.03.014, **2011**.